SYNTHESES, CHARACTERISATION AND MESOPHASE INVESTIGATION OF A NEW CLASS OF HYDRAZINE-BASED LIQUID CRYSTAL DIMERS

UMAIRAH BINTI ABD RANI

UNIVERSITI SAINS MALAYSIA
2016

SYNTHESES, CHARACTERISATION AND MESOPHASE INVESTIGATION OF A NEW CLASS OF HYDRAZINE-BASED LIQUID CRYSTAL DIMERS

By

UMAIRAH BINTI ABD RANI

Thesis submitted in fulfillment of the requirements
for the degree of
Master of Science

February 2016

ACKNOWLEDGEMENT

Firstly, I'm so thankful and praise Allah the Almighty for His generosity of blessings. I would like to express my highest appreciation to my main supervisor, Dr Yam Wan Sinn for her teaching, supervision, advice and attention throughout the period of my candidature. I also wish to thank the Dean, Professor Wan Ahmad Kamil Mahmood and staff of School of Chemical Sciences for support and providing me with the research facilities and services.

I wish to thank Professor Ewa Gorecka of Warsaw University, Poland, and Dr. Krishna Prasad of the Centre for Soft Matter Research, India for their assistance in X-ray diffraction analyses. Also, I would like to express my appreciation to Dr Yip Foo Win of Universiti Tunku Abdul Rahman (UTAR) for conducting the DSC measurements. I am so grateful to my laboratory mate, Goh Yit Peng for assisting and providing me with moral support in many aspects at the work place.

To my family and all my friends, I wish to express my best regards and gratitude for their prayers and support.

TABLE OF CONTENTS

LIST OF TABLES

LIST OF FIGURES

LIST OF ABBREVIATION

$^{o}C\ min^{-1}$	Degree Celcius per minute
^{1}H-NMR	Proton nuclear magnetic resonance
^{13}C-NMR	Carbon nuclear magnetic resonance
$Å\ K^{-1}$	Angstrom per Kelvin
$CDCl_3$	Deuterated chloroform
CHN	Carbon, hydrogen and nitrogen
COSY	Correlation spectroscopy
Cr	Crystal
d	Doublet
dd	Doublet of doublet
DCC	N,N-dicyclohexylcarbodimide
DCM	Dichloromethane
DEPT	Distortionless enhancement by polarisation transfer
DMAP	4-dimethylaminopyridine
DMF	Dimethylformamide
DSC	Differential scanning calorimetry
FT-IR	Fourier transform infrared
FT-NMR	Fourier transform nuclear magnetic resonance

HMBC	Heteronuclear multiple bond correlation
HMQC	Heteronuclear multiple quantum correlation
Iso	Isotropic phase
J	Coupling constant
kJ mol^{-1}	Kilojoule per mole
L	Molecular length
LC	Liquid crystal
m	Multiplet
MHz	MegaHertz
n	Number of methylene units
N	Nematic phase
N*	Chiral nematic phase
POM	Polarising optical microscope
s	Singlet
SmA	Smectic A phase
SmA*	Chiral smectic A phase
SmB	Smectic B phase
SmC	Smectic C phase
SmC*	Chiral smectic C phase

SmJ	Smectic J phase
t	Triplet
T_c	Clearing temperature
T_m	Melting temperature
THF	Tetrahydrofuran
TMS	Tetramethylsilane
v/v	Volume per volume
XRD	X-ray diffraction
δ/ppm	Chemical shift in part per million unit
ν/cm^{-1}	Wavenumber per centimeter unit
z	Layer normal

SINTESIS, PENCIRIAN DAN KAJIAN CIRI FASA BAGI SUATU KELAS BARU HABLUR CECAIR DIMER BERDASARKAN HIDRAZINA

ABSTRAK

Empat siri baru hablur cecair dimer tak simetri yang berdasarkan dibenzilidinahidrazina, *N*-{4[10-(16-desiloksifenilimino) metil)fenoksi] alkiloksibenzilidina}-*N*'-(4'-desiloksibenzilidina)hidrazina **(SB-$(CH_2)_n$-HZ)**, *N*-{4[10-(16-desiloksifenildiazenil)fenoksi]alkiloksibenzilidina}-*N*'-(4'-desiloksibenzilidina) hidrazine **(AZ-$(CH_2)_n$-HZ)**, *N*-[4-{12-[18-((*S*)-(-)-23-metilbutiloksi)karbonilfenil]fenoksi}alkiloksibenzilidina]-*N*'-(4'-desiloksibenzilidina)hidrazina **(BP-$(CH_2)_n$-HZ)** dan *N*-(4-alkiloksibenzilidina)-*N*'-[4'-(kolesteriloksikarbonil)alkiloksibenzilidina]hidrazina **(Chol-$(CH_2)_m$-HZ-$(CH_2)_n$)** telah disintesis dan dicirikan. Kesemua dimer ini mengandungi dibenzilidinahidrazina sebagai salah satu kumpulan mesogenik dan berbeza antara satu sama lain dari segi cabang sisi dan panjang spaser. Struktur molekul bagi dimer tersebut telah dijelaskan oleh analisis CHN, spektroskopi FT-IR, 1D dan 2D-NMR. Ciri hablur cecair dimer ini telah dikaji dengan menggunakan POM, DSC dan XRD. Sifat fasa bagi kesemua dimer ini didapati bergantung pada struktur dan kepanjangan spaser. Pelbagai jenis fasa termasuklah fasa nematik (N), kolesterik (N*), smektik A (SmA), smektik A kiral (SmA*), smektik C (SmC), smektik C kiral (SmC*) dan smektik J (SmJ) telah diperhatikan apabila kumpulan mesogenik di salah satu cabang sisi telah diubah. Kesan ganjil-genap yang ketara dalam ciri peralihan (suhu peleburan, suhu penjernihan dan perubahan entropi) dapat diperhatikan dalam **SB-$(CH_2)_n$-HZ, AZ-$(CH_2)_n$-HZ** dan **BP-$(CH_2)_n$-HZ** apabila kepanjangan spaser berubah.

SYNTHESES, CHARACTERISATION AND MESOPHASE INVESTIGATION OF A NEW CLASS OF HYDRAZINE-BASED LIQUID CRYSTAL DIMERS

ABSTRACT

Four new series of non-symmetric dibenzylidenehydrazine-based liquid crystal dimers, *N*-{4[10-(16-decyloxyphenylimino)methyl)phenoxy] alkyloxybenzylidene}-*N*'-(4'-decyloxybenzylidene)hydrazines **(SB-$(CH_2)_n$-HZ)**, *N*-{4[10-(16-decyloxyphenyldiazenyl)phenoxy]alkyloxybenzylidene}-*N*'-(4'-decyloxybenzylidene) hydrazines **(AZ-$(CH_2)_n$-HZ)**, *N*-[4-{12-[18-((*S*)-(-)-23-methylbutyloxy)carbonylphenyl] phenoxy} alkyloxybenzylidene]-*N*'-(4'-decyloxybenzylidene) hydrazines **(BP-$(CH_2)_n$-HZ)** and *N*-(4-alkylxybenzylidene)-*N*'-[4'-(cholesteryloxycarbonyl)alkyloxybenzylidene]hydrazines **(Chol-$(CH_2)_m$-HZ-$(CH_2)_n$)** had been synthesised and characterised. All dimers incorporated dibenzylidenehydrazine as one of the mesogenic arms and differ in terms of the other side arms and spacer parity. The molecular structures of these dimers were elucidated by CHN, FT-IR, 1D and 2D-NMR spectroscopy. Their liquid crystalline properties were investigated using POM, DSC and XRD. Phase behavior of the dimers was structure and spacer parity dependent. Various mesophases including nematic (N), cholesteric (N*), smectic A (SmA), chiral smectic A (SmA*), smectic C (SmC), chiral smectic C (SmC*) and smectic J (SmJ) were observed when one of the mesogenic side arms was changed. A pronounced odd-even effect in transitional properties (melting and clearing temperatures as well as entropy changes) were seen in **SB-$(CH_2)_n$-HZ, AZ-$(CH_2)_n$-HZ** and **BP-$(CH_2)_n$-HZ** upon varying the spacer length.

1.0 INTRODUCTION

1.1 Liquid crystals

The study of liquid crystals (LCs) began in 1888 by an Austrian botanist named Friedrich Reinitzer. In his study, he extracted cholesteryl benzoate from carrots and observed that it melted into a cloudy liquid at 145.5 ºC. When the temperature reached 178.5 ºC, the cloudy liquid suddenly became clear (Reinitzer, 1888). Later, a German physicist named Lehmann examined this cloudy liquid using a polarised optical microscope and observed the optical anisotropy of a new liquid state. He suggested that this cloudy liquid had to be a new state of matter and hence he termed it as liquid crystal (Broer, 1989).

Liquid crystalline material is an intermediate state of matter between a crystalline solid and an isotropic liquid. In a solid state, molecules are highly ordered and have no translational freedom. However, molecules in a liquid crystalline state have a tendency to point along a common axis, known as a director, *n*. This condition is in contrast to molecules in a liquid phase, in which they have no intrinsic order and are randomly distributed. The arrangement of molecules in each of the aforementioned state is represented in Figure 1.1.

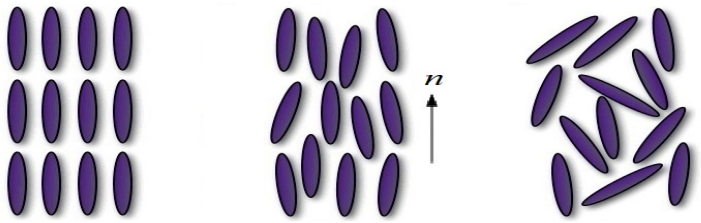

Figure 1.1: Arrangement of molecules in three different states of matter (Shakhashiri, 2007).

1.2 Types of liquid crystals

According to the literature, LC phases or mesophases can be induced either by the addition of solvent or by varying the temperature. Therefore, LCs can be classified into two general categories: (i) thermotropic LCs in which phase transitions are thermally induced, and they exhibit one or more anisotropic mesophases between melting and clearing temperatures; (ii) lyotropic LCs, where phase transitions happen as a result of solvent-induced aggregation of the essential mesogens into micellar structures and they exhibit LC properties in a certain concentration range. However, this study focuses only on the investigation of phase behaviour of thermotropic LCs and hence, lyotropic LCs will not be discussed further.

1.3 Mesophases

The term mesophase is used to elaborate the sub-phases of liquid crystalline materials (Friedel, 1922). The two major types of mesophases are nematic (N) and smectic (Sm) phases. However, many other mesophases have also been discovered in hitherto reported literatures such as the frustrated, cubic (discotic) and banana phases (Manickam and Kumar, 1998; Bushby and Kawata, 2011).

1.3.1 Nematic phase

The least ordered mesophase is the nematic (N) phase. It has fluidity similar to isotropic liquids. The molecules in this phase have only orientational order but no positional order. Molecules in a N phase tend to align themselves towards a similar direction referred to as the director, *n* (Figure 1.2) (Seideman, 1990).

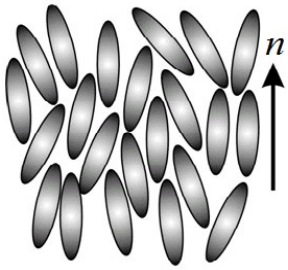

Figure 1.2: Molecular arrangement in a N phase (Carsten and Demetri, 2010).

1.3.1.1 Cholesteric phase

This phase is also known as a chiral nematic (N*) phase. This mesophase is exhibited by materials composed of optically active molecules. Molecules in a cholesteric phase are orientationally ordered, but rotationally disordered in a direction perpendicular to the plane. Therefore, molecules in this phase form a helical structure which has a helical axis perpendicular to the director, *n* (Figure 1.3) (Raju *et al*., 1999).

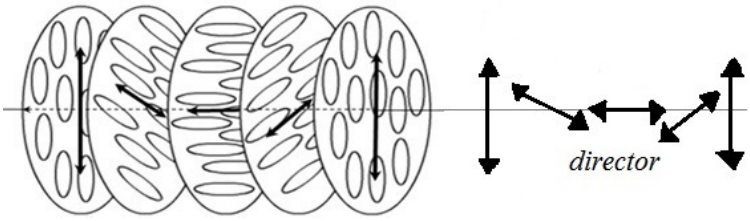

Figure 1.3: Molecular arrangement of a N* phase. The handedness causes the director orientation to rotate slightly between the layers.

1.3.2 Twist grain boundary phases

Twist grain boundary (TGB) phases were first predicted theoretically by Renn and Lubensky (1988). They are generally observed in the temperature range between a cholesteric phase and a smectic phase.

This phase was formed by rotated blocks of SmA* layers in which the long molecular axes are arranged perpendicular to the layer planes, while the TGB helix axis is perpendicular to the local director. The structure of a TGBA* phase is shown in Figure 1.4 in which it comprises of smectic slabs (1_b), separated by defect walls (grain boundaries) consisting of defect lines (screw dislocations). In the slabs, molecules are arranged in layers with their director normal to the smectic layers. Hitherto reported TGB phases include TGBA*, TGBC* and undulated TGB phases (Lavrentovich *et al*., 1990).

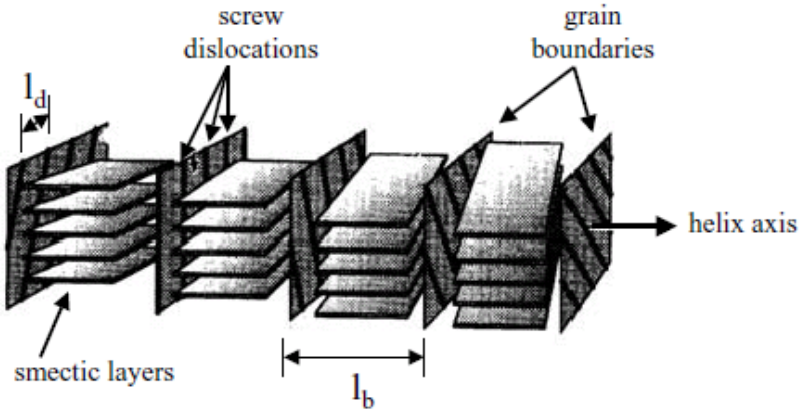

Figure 1.4: Schematic representation of TGBA* phase (Pandey *et al*., 2008).

1.3.3 Smectic phases

Molecules in smectic phases are arranged in layers. They show a degree of translational order and maintain the general orientational order of a nematic phase. Within each layer, the molecules diffuse freely over one another just as in ordinary liquids. However, translation of molecules form one layer to another is limited. A diversity of molecular arrangements is possible within these layers.

1.3.3.1 Smectic A phase

The simplest least ordered smectic phase. Molecules in a SmA phase are orthogonal to the layer plane with no positional order within layers and the long axes (Figure 1.5 (a)) (Mcmillan, 1971).

1.3.3.2 Smectic C phase

The molecular arrangement in a smectic C (SmC) phase is closely related to that of the SmA phase, in which the molecules in both phases are arranged in layers. However, the preferred axis in a SmC phase is not perpendicular to the layers. The long axes of the molecules in this phase are tilted at an angel, θ with respect to the layer normal, z (Figure 1.5 (b)). Hence, this phase has a biaxial symmetry with a new director, n (Goodby and Gray, 1979).

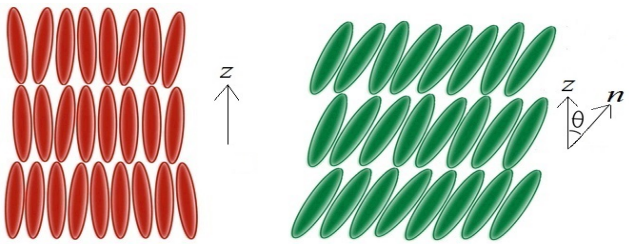

(a) (b)

Figure 1.5: Molecular arrangements in (a) SmA and (b) SmC phases (Dierking, 2003).

1.3.3.3 Hexatic smectic phases

Molecules in hexatic smectic phases possess bond orientational order in which the centres of mass of molecules are arranged on an orientated hexagonal net (Figure 1.6). Within a smectic layer, long range orientational and short range positional ordering could be seen.

Hence, the hexagonal structures have no interlayer positional correlation (Dierking, 2003). SmB, SmI and SmF are the three different hexatic smectic phases. SmB phase is also known as the orthogonal hexatic smectic phase wherein the molecules within layers are arranged in close-packed hexagons with the director perpendicular to the layer planes (Gray and Goodby, 1999). SmI and SmB phases, the two tilted versions of the hexatic smectic phases, differ from each other in the direction of tilt of the molecules. Molecules in SmI phase are tilted towards the apex of the hexagon whilst in SmF phase, the molecules tilt to the side. The model structures of the three hexatic smectic phases are shown in Figure 1.7.

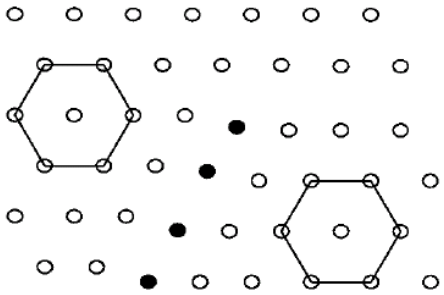

Figure 1.6: Bond-orientational order in hexatic smectic phases (Dierking, 2003).

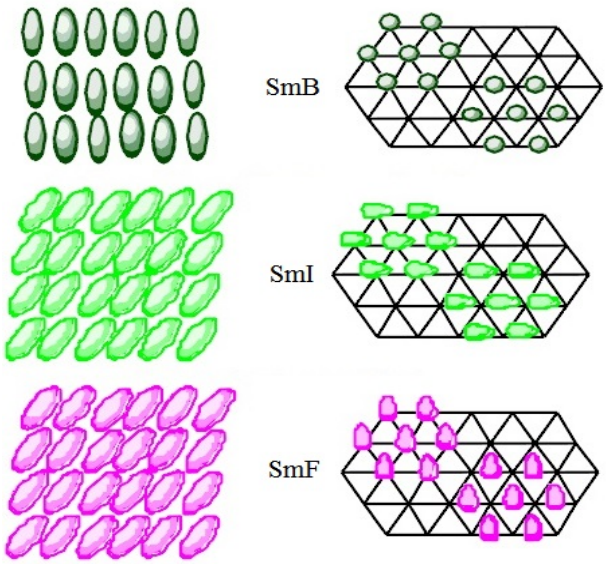

Figure 1.7: Model structures of hexatic smectic phases (Goodby *et al*., 1999).

1.3.3.4 Chiral smectic phase

The presence of one or several chiral centres in mesogenic molecules can modify the organisation of a mesophase. For example, a chiral centre can induced a twisted orientational order in an otherwise untilted or tilted one which is present in achiral LC materials. For example, in the most common chiral SmC (SmC*) phase, the molecules are positioned in a layered structure and tilted at an angle, θ with respect to the layer normal. The precession of the tilted molecules gives rise to a macroscopic helical structure with the layer normal, *z* and the director, *n* (Figure 1.8). Interestingly, this helical structure has a spontaneous polarization (*Ps*) in which every layer has a permanent dipole moment perpendicular to the plane defined by the layer normal and the local director. This phase is, in general, ferroelectric and has fast switching speeds as the orientation of the tilt can be altered by an external electric field (Silvia *et al*., 2011).

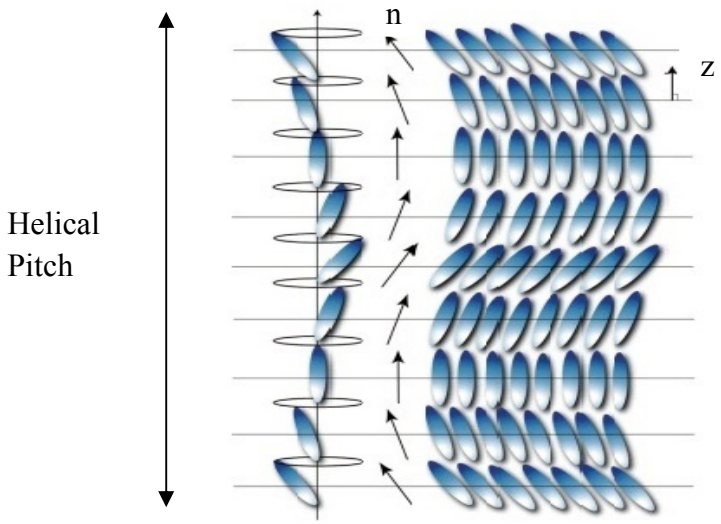

Figure 1.8: A helical structure of a SmC* phase (Alison *et al*., 2006).

1.3.4 Soft crystal phases

The molecular arrangements in soft crystal B, J and G phases are analogous to those of hexatic SmB, SmI and SmF phases, respectively. The only difference between the two is the presence of long range positional order in soft crystal phases. The structures of crystal E, K and H phases, on the other hand, are of a herringbone-type which resulted from a strong hindrance of molecular rotational around the long axis. The E phase is orthogonal with an orthorhombic unit cell. Both the K and H phases have a monoclinic unit cell with molecules in the former tilted to side *a* and those in the latter tilted to side *b* (Figure 1.9) (Gray and Goodby, 1999).

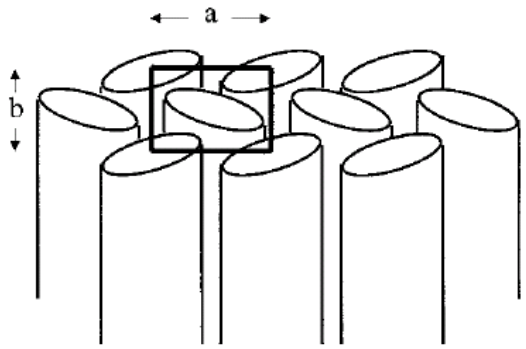

Figure 1.9: Model structure of the orthorhombic soft crystal E phase (Dierking, 2003).

2.0 Literature Review

2.1 Liquid crystal dimers

Research in LC dimers started in the early 1920s and the first LC dimer was discovered by Vorlander, (1927). However, the investigation of LC dimers was overlooked until the 1970s. The study on this class of LCs was revived by Rault and co-workers (1975). This special class of LCs is interesting not only because they can serve as model compounds for semi-flexible main chain liquid crystal polymers, but also of their unique thermal properties as compared with conventional low molar mass mesogens. LC dimers can be divided into two classes: symmetric and non-symmetric. A symmetric LC dimer consists of two identical mesogenic units linked *via* a flexible spacer whereas a non-symmetrical dimer is formed by two different mesogenic moieties connected through a flexible spacer. Figure 2.1 shows the general structural template of a LC dimer with A and B as the mesogenic moieties, X as the spacer and Y as the terminal chains.

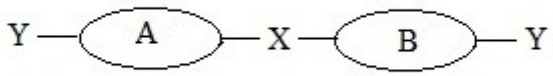

Figure 2.1: General structural template of a LC dimer.

2.2 Structure-property relationship of liquid crystal dimers

2.2.1 Phase behaviour of liquid crystal dimers

Smectic behaviour in LC dimers is strongly dependant on the parity of the flexible spacer and the length of the terminal chains. When the terminal chains are longer than half the spacer length, smectic phases are observed (Date *et al*., 1992). However, when the spacer length is increased, so is the tendency for LC dimers to form nematic phases instead of smectic phases. This behaviour was observed for symmetric and non-symmetric LC dimers (Date *et al*., 1992; Blatch and Luckhurst, 2000). For example, symmetrical LC dimers, α,ω-bis{4-[(2-hydroxy-4-*n*-octyloxy phenyl)iminomethyl]phenyloxy}alkanes with long spacer exhibited a nematic phase (Yelamaggad *et al*., 2003). Attard and co-workers (1994) also reported that in a series of non-symmetrical LC dimers, α-(4-cyanobiphenyl-4'-yloxy)-ω-(4-*n*-alkylanil inebenzylidene-4'-oxy)alkanes, homologues with shorter spacer exhibited smectic phases while nematic phase was seen when the length of the spacer was increased.

In addition to the spacer parity and terminal chain length, it had been reported by Sato and Ujiie (1996) that the phase behaviour of LC dimers is also dependant on the type of terminal groups. For example, in 1,8-bis[5-(4-substituted-phenyl)-1,3,4-oxadiazolyl-2-phenoxy]octanes, a series of oxadiazole derived symmetrical LC dimers containing different terminal substituents, all homologues with electron-withdrawing terminal groups were found to exhibit enantiotropic nematic phases while those with electron-donating terminal groups showed no liquid crystalline behaviour.

Similar observation was also reported by Jie Han and co-workers (2010) in a series of unsymmetrical liquid crystal dimers, 2-(4-substitutedphenyl)-5-(4-(10-(4'-fluorobiphenyl-4-yloxy)decyloxy)phenyl)-1,3,4-oxadiazoles in which homologue bearing the strongly polar cyano group tend to form more stable mesophases. The rationale was it formed more conjugated structure with the mesogenic core, thus resulting in a larger dipole across the molecular axis which is good in stabilising the molecular orientation which is essential for the generation of mesophases (Kumar, 2001). The fluorinated and methoxylated homologues, on the other hand, exhibited enantiotropic or monotropic N and monotropic SmA phases.

2.2.2 Layer arrangement of smectic phase in liquid crystal dimers

In general, symmetric LC dimers have potent tendency to exhibit monolayer smectic phases (Figure 2.2 (a)) whilst intercalated or interdigitated smectic organisation are usually observed in non-symmetric LC dimers. In monolayer smectic arrangement, the smectic layer periodicity, *d* is almost approximately equal to the molecular length, *L* ($d/L \approx 1$) (Attard *et al*., 1994). The intercalated smectic phase (Figure 2.2 (b)), on the other hand, was formed when the spacer is longer than the terminal chains. The smectic periodicity, *d* in this phase is approximately half the molecular length, *L* ($d/L \approx 0.5$) (Blatch *et al*., 1992; Marcelis *et al*., 2001). Hogan and co-workers (1988) proposed that the intercalated smectic phases may be stabilised by the interaction between different mesogenic groups as seen in non-symmetric LC dimers incorporated a cyanobiphenyl and alkylanilinebenzylidene moieties. Another stabilising factor of this phase is the electrostatic quadrupolar interaction between two distinct mesogenic moieties possessing quadrupolar moments of opposite signs (Blatch *et al*., 1995). One of the reported series of

unsymmetric dimers to exhibit such a phase is the α-(4-alkylanilinebenzylidene-4'-oxy)-ω-(4-cyanobiphenyl-4'-yloxy)alkanes, in which the intercalated arrangement was postulated to be stabilised by a favourable charge-transfer interaction between the cyanobiphenyl and Schiff base groups (Attard *et al*., 1994). In some cases, symmetric LC dimers were also found to exhibit intercalated smectic phase. For example, in α,ω-bis (4,4'-butoxybiphenylcarbonyloxy)alkanes, the even-membered homologues exhibited intercalated SmA phase, while the odd-membered counterparts formed intercalated SmC phase (Watanabe and Komura, 1993).

However, when the terminal chains are longer than the spacer, the molecules adopt an antiparallel arrangement, thus resulting in the formation of an interdigitated smectic phase (Figure 2.2 (c)) where compatible parts of the molecules overlap. The layer thickness of this phase, d is longer than the length of one molecule but shorter than that of two molecules: $L < d < 2L$ (Attard *et al*., 1994). This molecular arrangement is stabilised by the electrostatic interactions between two mesogenic groups. The large difference in steric bulk between the mesogenic groups such as the cholesteryl and cyanobiphenyl groups also play an important role in stabilising this phase (Imrie, 1999). For example, all homologues in a series of non-symmetric LC dimers consisiting of a cholesteryl and 4-cyanobiphenyl moieties, CN-*n*-Chol, formed an interdigitated SmA phase which is stabilised by the electrostatic interaction between the polar and polarisable cyanobiphenyl groups (Donaldson *et al*., 2010).

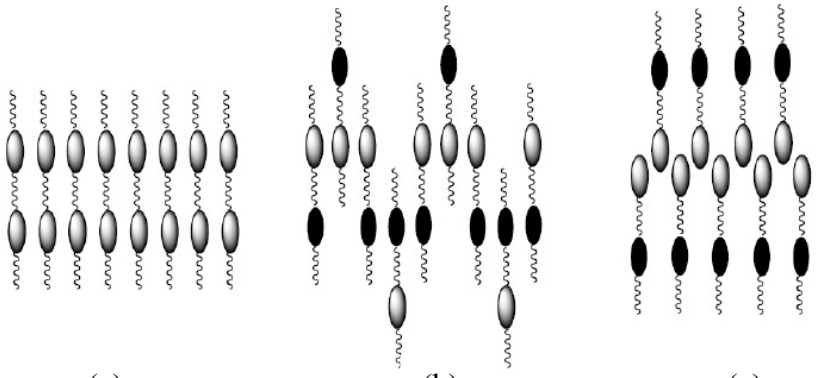

(a) (b) (c)

Figure 2.2: Diagramatic representations of SmA arrangement in LC dimers, (a) monolayer, (b) intercalated, and (c) interdigitated (Imrie and Henderson, 2002).

2.2.3 Odd-even effect in liquid crystal dimers

An archetypal behaviour of LC dimers is their ability to exhibit significant odd-even effects in transitional properties due to a variation of parity which results in a conformational constraint of the molecules (Imrie, 1999). When considered in their all-*trans* conformation, LC dimers with even-parity spacer are arranged in an anti-parallel manner and they adopt a zig-zag conformation (Figures 2.3 (a)). Therefore, the shape anisotropy of the dimers is enhanced and this in turn, allows them to pack more efficiently in a crystal lattice and mesophase, thus resulting in higher phase transition temperatures and entropy change. For example, a pronounced odd-even effect was observed in α-(4'-alkylazobenzene-4-oxy)-ω-(4'-alkylazobenzene-4-oxy)alkanes, wherein the even-parity homologues possessed higher phase transition temperatures, T_{SmA-N} and T_{N-I} as compared to their odd-counterparts (Blatch and Luckhurst, 2000). On the other hand, in odd-parity dimers, the two mesogenic units are inclined at some angle with respect to each other, hence, they tend to adopt a bent conformation (Figure 2.3 (b)) and thus, their packing efficiency is reduced.

Consequently, they have lower phase transition temperatures and entropy change (Henderson *et al*., 2001; Imrie and Luckhurst, 1998). However, attenuation in odd-even effect is often observed in the clearing temperatures, T_C of the dimers on increasing the spacer length. This indicates that the number of possible conformations also increases and the average molecular shapes of odd and even-parity segments become more similar (Imrie *et al*., 2001).

(a) (b)

Figure 2.3: Molecular shapes of LC dimers with (a) even-parity, and (b) odd-parity spacer when considered in all-*trans* conformations.

Contrary to many LC dimers containing ether, alkane and ester linkages which exhibited strong odd-even effects, there are exceptions to this characteristic behaviour where odd-even fluctuations in transitional properties were greatly reduced or totally disappeared. This phenomenon is usually observed in LC dimers containing carbonate linkage in the spacer. It can be explained based on a theoretical analysis derived from the rotational isomeric states (RIS) mean field approach. According to this model, distribution of conformers (linear versus bent) in carbonate LC dimers is insignificant as opposed to many ether and ester dimers in which the distinction in conformational distribution is great. Structural differences between these dimers were reported to be another possible contributing factor (Abe *et al*., 1995). In another study by Roberto (2009), odd-even fluctuation was reported to be absent in dimers with carbonate linkages. Small differences in terms of thermodynamic properties (for example ΔS and T_{NI}) of consecutive members of a

homologous series (from *n* to *n*+1, where *n* is the number of methylene units in the spacer) and distributions of conformers are believed to be the reasons for this observation.

Interestingly, odd-even effect was also observed in the phase behavior of LC dimers. For example, in α-(4-cyanobiphenyl-4'-yloxy)-ω-[4-(5-octylpyrimidine-2-yl)phenyl-4''-oxy]alkanes, SmC-SmA-N transitions were observed in homologues with odd-parity spacer whereas the even-membered homologues exhibited only the SmA-N phase sequence (Yoshizawa *et al*., 1998). It had also been documented that LC dimers with even-parity spacers exhibited SmA and/or N phases while compounds with odd-parity exhibited SmC phases (Kim *et al*., 2007). Ewa and co-workers (2008) also reported that in a series of symmetrical LC dimers, α,ω-alkanedicarboxylic acids 4'-decyloxybiphenyl diesters, in which tilted SmC phases were seen in even-parity homologues while the odd-parity homologues exhibited the B4 phase. Furthermore, according to Wang and co-workers (2008), odd-membered homologues in α,ω-bis[*N*-(4-hexadecyloxybenzoyl)-*N*'-benzoyl-4'-oxy)hydrazine] alkanes exhibited SmA phases whereas SmC phase was seen in the even-membered homologues. In 2010, Yutaro and Atsushi reported that homologues with even-spacers in (*R*)-2,2'-bis{6-[4-(4-(4-hexylphenyl)-2,3-difluorophenyl)phenyl oxycarbonyl]alkyloxy}-1,1-binaphthyl were found to induce left-handed helical structures with a short pitch whereas their odd-spacer counterparts exhibited temperature-dependent helical twist inversion.

2.2.4 Chirality effect on liquid crystalline properties of dimers

The study of chiral LCs was discovered more than 100 years ago (Renitzer, 1888). The presence of chiral centres either in the terminal chain(s) or spacer(s) tends to modify the molecular arrangement of mesophases. Cholesterol, for example, is one of the most widely incorporated chiral mesogenic moieties in LC dimers as these dimers often exhibit a rich variety of mesophases (Imrie, 1999; Yelamaggad *et al*., 2008). For example, a series of cholesteryl–based symmetrical chiral LC dimers were found to exhibit TGB, N* and monotropic SmC* phases. All homologues with even-parity spacer showed well-ordered N* phases, thus leading to a higher N*-I transition as well as higher enthalpy values (Yelamaggad and Shanker, 2007). Re-entrant TGB_A^* and TGB_{C*} phases were seen in non-symmetrical chiral dimers incorporating a cholesteryl ester and -*n*-hexyloxytolane moieties linked *via* a *n*-pentyl spacer (Prasad *et al*., 2001).

2.3 Hydrazine-based non-symmetrical liquid crystal dimers

Schiff bases are generally prepared by condensation reactions of primary amines with active carbonyls. Aromatic imine compounds with rod-like structure are well known for their ability to exhibit liquid crystalline behaviour resulted from their anisotropy shape. Many studies on LC dimers containing Schiff base moieties had been reported as they were found to display a generous smectic polymorphism (Date *et al*., 1992). Similar to Schiff bases, the dibenzylidenehydrazine moiety, a derivative of hydrazine, contains two imino groups (C=N) connected *via* an azine (N-N) linkage. A literature search revealed very little of published data on the chemical and optical properties of thermotropic LCs dimers derived from hydrazine except for a series of symmetrical LC dimers,

1,*n*-alkanoic acid, bis{4-[1-[[1-[4-(acetyloxy)phenyl]ethylidine]hydrazono]ethyl] phenyl}esters. These thermotropic nematogens showed odd-even fluctuations in the transitional properties (Roberto *et al*., 2006). Hence, we are prompted to investigate the phase properties of hydrazine-based LC dimers with various structural modifications.

2.4 Research objectives

The objectives of this study are:

i. To synthesise a new class of hydrazine-based non-symmetric liquid crystal dimers

ii. To characterise the synthetic compounds using various spectroscopic techniques such as FT-IR, 1D and 2D NMR spectroscopy and CHN microanalyses.

iii. To investigate the phase behaviour of the synthetic compounds using DSC, POM and X-ray diffraction.

3.0 EXPERIMENTAL

3.1 Chemicals

From Acros Organic, Belgium: 4-acetamidophenol, 98%; 1-bromodecane, 98%; hydrazinium sulphate, 97%; 1,12-dibromododecane, 96% and dicyclohexylcarboiimide, 99%. From Qrec, Asia: sodium hydroxide pellets, 99%; calcium chloride anhydrous, 95%; glacial acetic acid, 99% and potassium carbonate, 99%. From Merck, Germany: 4-hydroxybenzaldehyde, 98%; hydrochloric acid, 37%; 1,3-dibromopropane, 99%; 1,4-dibromobutane, 98%; 1,5-dibromopentane, 97%; 1,6-dibromohexane, 97%; 1,8-dibromooctane, 97%; 4-dimethylaminopyridine, 99%; 4-bromobutane, 98%; 6-bromohexane, 98%; 8-bromooctane, 98% and 12-bromododecane, 98%. From Sigma-Aldrich, United States of America: 1,7-dibromoheptane, 97%; 1,9-dibromonone, 97%; 1,10-dibromodecane, 97%; 1,11-dibromoundecane, 98%; 4-(4-hydroxyphenyl)benzoic acid, 99%; 2-methyl-1-butanol, 95%; 5-bromopentanoic acid, 97% and 10-bromodecanoic acid, 95%. From Fluka, Switzerland: sodium acetate anhydrous, 96% and sodium nitrate, 96%. From R & M Chemical, United Kingdom: phenol 96%. From Tokyo Chemical Industry, Japan: cholesterol, 95%. All chemicals were used without further purification unless stated otherwise.

3.2 Syntheses of *N*-{4[10-(16-decyloxyphenylimino)methyl)phenoxy]alkyloxy benzylidene}-*N*'-(4'-decyloxybenzylidene)hydrazines, SB-$(CH_2)_n$-HZ (n = 3-12)

The aforementioned compounds were synthesised according to the synthetic routes shown in Scheme 1.

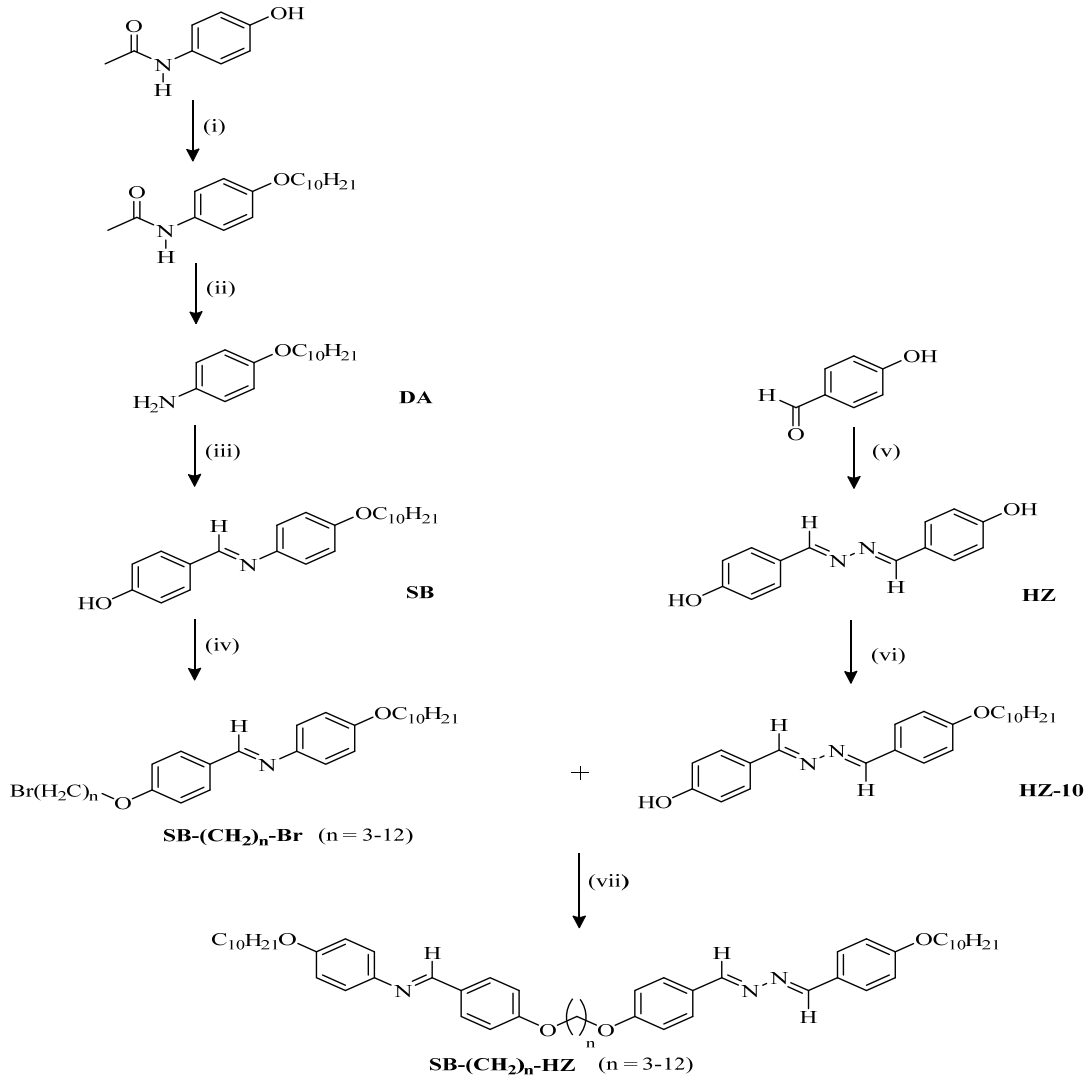

Scheme 1: Reagents and conditions: (i) 1-bromodecane (1.1 equiv.), K_2CO_3 (3.0 equiv.), refluxing in acetone, 48 h; (ii) refluxing in HCl_{conc} and EtOH (1:2,v/v), 4 h; (iii) 4-hydroxybenzaldehyde (1.5 equiv.), glacial acetic acid (5 drops), refluxing in EtOH, 6 h; (iv) dibromoalkanes, $BrC_nH_{2n}Br$ (3.0 equiv.) (*n* = 3-12), K_2CO_3 (3.0 equiv.), refluxing in acetone, 6 h; (v) hydrazine solution, HCl_{conc} (dropwise), 50 ºC, 3 h; (vi) 1-bromodecane (0.5 equiv.), K_2CO_3 (3.0 equiv.), DMF, 80 ºC, 6 h; (vii) K_2CO_3 (3.0 equiv.), refluxing in acetone, overnight.

3.2.1 Synthesis of 4-decyloxyaniline, DA

DA was prepared via the method reported by Robert and Richard (1985) with some modifications. 4-Acetamidophenol (5.00 g, 32.98 mmol) was first dissolved in acetone (100 mL) in a 250-mL single-neck round bottom flask. Anhydrous potassium carbonate (3.0 equiv., 98.94 mmol) was then added. Subsequently, 1-bromodecane (1.1 equiv., 36.28 mmol) was added to this solution. The reaction mixture was refluxed for two days. The resultant mixture was cooled to room temperature and excess solvent was removed via evaporation. The crude product was then washed with hexane to get rid of excess 1-bromodecane. The resultant mixture was filtered and the residue was collected. It was then added to a mixture of concentrated hydrochloric acid and ethanol (1:2, v/v) in a 250-mL round bottom flask and the reaction mixture was refluxed for 4 hours. The resultant solution was cooled to room temperature and ethanol was removed *via* a rotary evaporator, thereafter it was transferred to a separating funnel. It was then extracted with dichloromethane and water (1:1, v/v). The aqueous layer was removed and the organic layer was dried with anhydrous calcium chloride. Calcium chloride was then removed *via* filtration and excess solvent was removed in *vacuo* upon which a white precipitate was formed. The crude product was recrystallised from a solution of ethanol and dichloromethane (1:1, v/v). Yield: 89 %. Melting point: 162-164 ºC. IR (KBr) ν/cm^{-1}: 3320 (N-H), 2849 ($CH_{2\ sym}$), 2920 ($CH_{2\ asym}$), 1608 (C=C aromatic), 1250 (C-O).

3.2.2 Synthesis of 4-(4'-decyloxyphenyliminomethyl)phenol, SB

SB was synthesised according to the method reported by Narayana and Durga (2009) with some modifications. In a 100-mL single-neck round bottom flask, **DA**

(3.00 g, 12.05 mmol) was mixed with 4-hydroxybenzaldehyde (1.5 equiv., 18.08 mmol) in ethanol (30 mL). Glacial acetic acid (5 drops) was then added to the reaction mixture and it was refluxed for 6 hours. The resultant mixture was then cooled to room temperature and excess solvent was removed via evaporation. The yellow precipitate obtained was recrystallised from diethyl ether to yield the titled compound. Yield: 90 %. Melting point: 141-143 ºC. IR (KBr) ν/cm^{-1}: 3400 (OH), 2850 ($CH_{2\ sym}$), 2919 ($CH_{2\ asym}$), 1622 (C=N), 1606 (C=C aromatic), 1257 (C-O). ^{1}H-NMR 500 MHz ($CDCl_3$) δ/ppm: 0.86 (*t*, 3H, J = 7.0 Hz, CH_3), 1.29-1.81 (*m*, 16H, CH_2), 4.25 (*t*, 2H, J = 6.5 Hz, OCH_2), 6.91 (*d*, 2H, J = 8.5 Hz, Ar-H), 7.03 (*d*, 2H, J = 8.5 Hz, Ar-H), 7.24 (*d*, 2H, J = 8.0 Hz, Ar-H), 7.45 (*d*, 2H, J = 8.5 Hz, Ar-H), 8.60 (*s*, 1H, CH=N).

3.2.3 Syntheses of 4'-bromoalkyloxybenzylidene-4-decyloxyanilines, SB-$(CH_2)_n$-Br (n = 3-12)

SB-$(CH_2)_n$-Br were prepared following a modified method reported by Satya and Monika (2004). In a 100-mL single-neck round bottom flask, **SB** (1.00 g, 2.83 mmol) was mixed with the corresponding dibromoalkane (3.0 equiv., 8.49 mmol) in acetone (20 mL). Anhydrous potassium carbonate (3.0 equiv., 8.49 mmol) was then added to this solution and the reaction mixture was refluxed for 6 hours. The resultant mixture was cooled to room temperature and excess solvent was removed *via* evaporation. Distilled water (30 mL) was then added to the mixture and the resultant precipitate was filtered and dried. The crude product was recrystallised from a solution of hexane and ethanol (1:1, v/v) to yield **SB-$(CH_2)_n$-Br** in their pure forms.

For *n* = 7, yield: 75 %. Melting point: 121-122 ºC. IR (KBr) *v*/cm^{-1}: 2853 ($CH_{2\ sym}$), 2917 ($CH_{2\ asym}$), 1623 (C=N), 1606 (C=C aromatic), 1256 (C-O). ^{1}H-NMR 500 MHz ($CDCl_3$) δ/ppm: 0.86 (*t*, 3H, *J* = 7.0 Hz, CH_3), 1.23-1.85 (*m*, 26H, CH_2), 3.27 (*t*, 2H, *J* = 6.5 Hz, CH_2Br) 4.23 (*t*, 2H, *J* = 6.5 Hz, OCH_2), 4.30 (*t*, 2H, *J* = 6.0 Hz, OCH_2), 7.02 (*d*, 2H, *J* = 7.0 Hz, Ar-H), 7.15 (*d*, 2H, *J* = 9.0 Hz, Ar-H), 7.20 (*d*, 2H, *J* = 8.0 Hz Ar-H), 7.40 (*d*, 2H, *J* = 8.5 Hz, Ar-H), 8.60 (*s*, 1H, CH=N). Other homologues showed similar spectral characteristics as those given for the aforementioned compound.

3.2.4 Synthesis of *N*, *N*'-bis(4-hydroxybenzylidene)hydrazine, HZ

HZ was prepared *via* the method reported by Graefe *et al* (1953) and Ashraf *et al* (2009) with some modifications. Finely powdered hydrazinium sulphate (1.00 g, 7.69 mmol) was suspended in a 250-mL beaker containing hot distilled water (20 mL). Anhydrous sodium acetate (8.00 g, 58.99 mmol) was then added to the suspension with stirring. The reaction mixture was boiled for 5 minutes, after which it was cooled to 50 ºC. Hot ethanol (50 mL) was then added to the reaction mixture and it was stirred for 5 minutes until an orange precipitate was formed. The precipitate was removed *via* filtration and the filtrate was added dropwise to an ethanolic solution of 4-hydroxybenzaldehyde (1.87 g, 15.32 mmol) in a 250-mL beaker. A few drops of hydrochloric acid were then added to this mixture and it was stirred on a water bath for 3 hours. The precipitate obtained was filtered and dried. The crude product was then recrystallised from absolute ethanol. Yield: 83 %. Melting point: 178-180 ºC. IR (KBr) *v*/cm^{-1}: 3320 (OH), 1623 (C=N), 1607 (C=C aromatic). ^{1}H-NMR 500 MHz ($CDCl_3$) δ/ppm: 7.15 (*d*, 4H, *J* = 8.0 Hz, Ar-H), 7.51 (*d*, 4H, *J* = 8.5 Hz, Ar-H), 8.42 (*s*, 2H, CH=N).

3.2.5 Synthesis of *N*-(4-hydroxybenzylidene)-*N*'-(4'-decyloxybenzylidene) hydrazine, HZ-10

In a 100-mL single-neck round bottom flask, **HZ** (1.80 g, 7.50 mmol) was mixed with 1-bromodecane (1.0 equiv., 7.50 mmol) in DMF (25 mL). Anhydrous potassium carbonate (3.0 equiv., 22.50 mmol) was then added to this solution and the reaction mixture was heated at 80 ºC for 6 hours in order to prevent decomposition of compounds (b.p of DMF = 153 ºC). Subsequently, the resultant mixture was poured into an ice water bath with rapid stirring upon which a yellow precipitate was formed. The crude product was filtered, dried and recrystallised from a solution of ethanol and hexane (1:1, v/v). Yield: 88 %. Melting point: 164-165 ºC. IR (KBr) ν/cm^{-1}: 3599 (OH), 2850 ($CH_{2\ sym}$), 2918 ($CH_{2\ asym}$), 1625 (C=N), 1608 (C=C aromatic), 1256 (C-O). ^{1}H-NMR 500 MHz ($CDCl_3$) δ/ppm: 0.87 (*t*, 3H, *J* = 7.5 Hz, CH_3), 1.23-1.82 (*m*, 16H, CH_2), 4.29 (*t*, 2H, *J* = 6.5 Hz, OCH_2), 7.14 (*d*, 2H, *J* = 8.0 Hz, Ar-H), 7.21 (*d*, 2H, *J* = 8.5 Hz, Ar-H), 7.48 (*d*, 2H, *J* = 8.5 Hz , Ar-H), 7.50 (*d*, 2H, *J* = 9.0 Hz, Ar-H), 8.42 (*s*, 2H, CH=N).

3.2.6 Syntheses of *N*-{4[10-(16-decyloxyphenylimino)methyl)phenoxy]alkyloxy-benzylidene}-*N*'-(4'-decyloxybenzylidene)hydrazines, SB-$(CH_2)_n$-HZ (n = 3-12)

In a 100-mL single-neck round bottom flask, **SB-$(CH_2)_n$-Br** (0.25 g, 0.53 mmol) and **HZ-10** (1.5 equiv., 0.79 mmol) were dissolved in acetone (30 mL). Anhydrous potassium carbonate (3.0 equiv., 1.59 mmol) was then added to this solution and the reaction mixture was refluxed overnight. The resultant mixture was cooled to room temperature and excess solvent was removed via evaporation. Distilled water (30 mL) was then added to the mixture upon which a light yellow precipitate was formed. The precipitate was filtered, dried and recrystallised from a

solution of acetone and chloroform (1:1, v/v). Spectral data of the titled compounds are given and discussed in Chapter 4.

3.3 Syntheses of *N*-{4[10-(16-decyloxyphenyldiazenyl)phenoxy]alkyloxy benzylidene}-*N*'-(4'-decyloxybenzylidene)hydrazines, AZ-$(CH_2)_n$-HZ (n = 3-12)

The aforementioned compounds were synthesised according to the synthetic routes shown in Scheme 2.

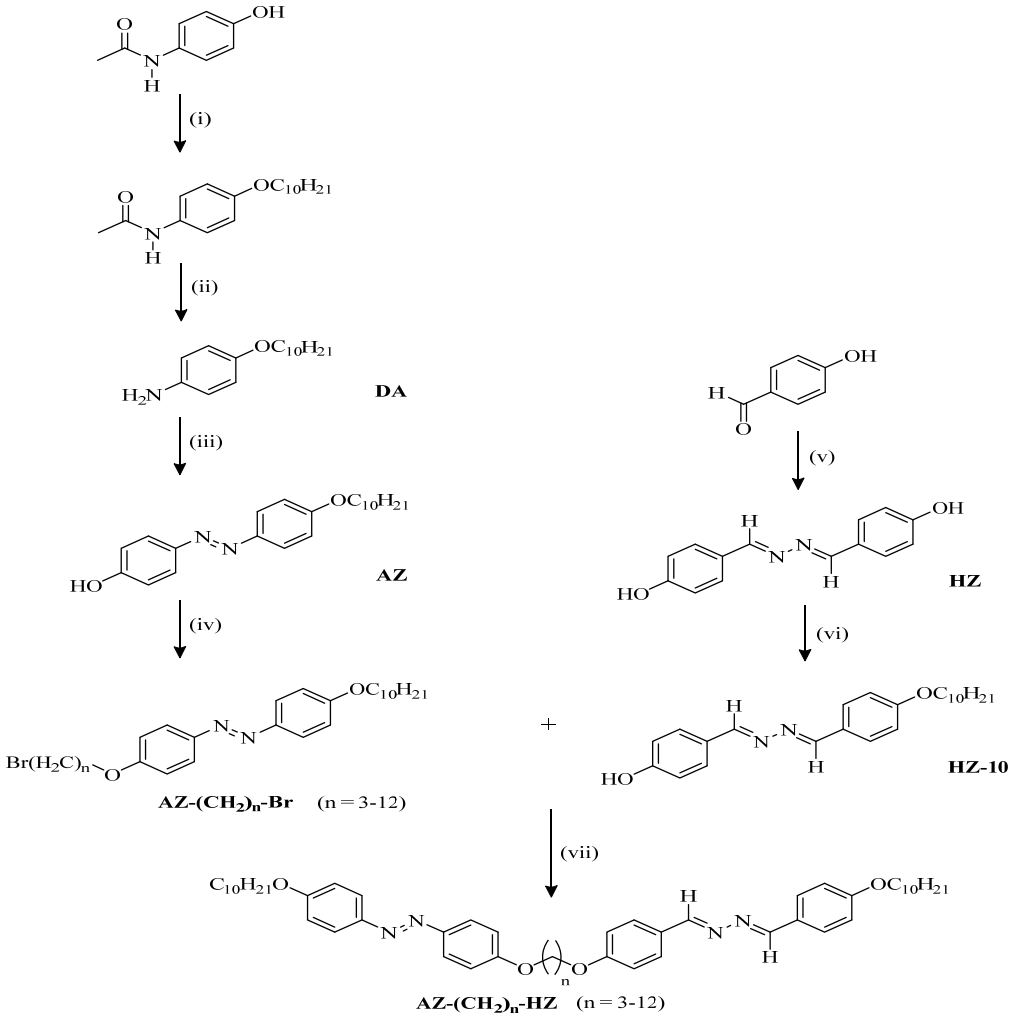

Scheme 2: Reagents and conditions: (i) 1-bromodecane (1.1 equiv.), K_2CO_3 (3.0 equiv.), refluxing in acetone, 48 h. (ii) refluxing in HCl_{conc} and EtOH (1:2,v/v), 4 h. (iii) $NaNO_2$ and phenol solution (1:1,v/v), NaOH (2%, w/v), $HCl_{conc,}$ (dropwise), stirring, 0 ºC, 3 h. (iv) dibromoalkanes, $BrC_nH_{2n}Br$ (3.0 equiv.) (*n* = 3-12), K_2CO_3 (3.0 equiv.), refluxing in acetone, 6 h. (v) hydrazine solution, $HCl_{conc,}$ (dropwise), 50 ºC, 3 h. (vi) 1-bromodecane (0.5 equiv.), K_2CO_3 (3.0 equiv.), DMF, 80 ºC, 6 h (vii) K_2CO_3 (3.0 equiv.), refluxing in acetone, overnight.